Published in final edited form as:
Neurobiol Aging. 2014 August ; 35(8): 1792–1800. doi:10.1016/j.neurobiolaging.2014.02.012.

Exosome Reduction *In Vivo* Is Associated with Lower Amyloid Plaque Load in the 5XFAD Mouse Model of Alzheimer's Disease

Michael B. Dinkins, **Somsankar Dasgupta**, **Guanghu Wang**, **Gu Zhu**, and **Erhard Bieberich**
Institute of Molecular Medicine and Genetics, Georgia Regents University, Augusta, Georgia 30912, USA

Abstract

We present evidence here that exosomes stimulate aggregation of Aβ1-42 *in vitro* and *in vivo* and interfere with uptake of Aβ by primary cultured astrocytes and microglia *in vitro*. Exosome secretion is prevented by inhibition of neutral sphingomyelinase 2 (nSMase2), a key regulatory enzyme generating ceramide from sphingomyelin, with GW4869. Using the 5XFAD mouse, we show that intraperitoneal injection of GW4869 reduces the levels of brain and serum exosomes, brain ceramide, and Aβ1-42 plaque load. Reduction of total Aβ1-42 as well as number of plaques in brain sections was significantly greater (40% reduction) in male than female mice. Our results suggest that GW4869 reduces amyloid plaque formation *in vivo* by preventing exosome secretion and identifies nSMase2 as potential drug target in AD by interfering with exosome secretion.

Keywords

Alzheimer's Disease; exosomes; amyloid beta; neutral sphingomyelinase; GW4869; astrocytes; primary culture

1. Introduction

Alzheimer's disease (AD) is characterized by cognitive decline, alteration of synaptic transmission, and neuronal death brought on by accumulation of neurofibrillary tangles in neurons and amyloid beta (Aβ) in the brain parenchyma. There is no viable therapy to slow or reverse AD progression. The leading hypothesis for the cause of AD is an impairment of clearance of Aβ resulting from the β-cleavage of the amyloid precursor protein (APP) (Bertram and Tanzi, 2008). Strong evidence comes from early-onset familial AD, in which patients carry mutations in genes encoding for APP or the presenilin-1 (PS1) component of

Correspondence to: Dr. Erhard Bieberich, Institute of Molecular Medicine and Genetics, Georgia Regents University, 1120 Fifteenth Street, CA-4054, Augusta, Georgia 30912, USA, Telephone: 1-706-721-9113, Fax: 1-706-721-8685, ebieberich@gru.edu.

Disclosure statement
The authors declare that they have no actual or potential conflicts of interest. All experiments involving animals followed approved protocols by Georgia Regents University's Institutional Animal Care and Use Committee.

the γ-secretase complex that cleaves APP to generate Aβ (Bird, 2008; Selkoe, 2011). Recent studies showing that reducing Aβ load in mouse models improves cognitive function strongly suggest that reducing plaque burden is a potential treatment strategy for AD (Cramer et al., 2012; Geekiyanage et al., 2013; Liu et al., 2013).

Exosomes are ceramide-enriched vesicles, 40–100 nm in diameter, generated by inward-budding of the endosomal membrane, and secreted when these multivesicular endosomes fuse with the plasma membrane (Thery, 2011; Trajkovic et al., 2008). Exosomes carry signaling factors and miRNAs that mediate intercellular communication, and there is evidence that exosomes play a role in the progression of AD (Bellingham et al., 2012). Aβ processing has been shown to be associated with endosomal compartments with a fraction of Aβ and C-terminal fragments being secreted in association with exosomes (Haass et al., 1995; Perez-Gonzalez et al., 2012; Rajendran et al., 2006; Sharples et al., 2008; Vassar et al., 1999). It is however unclear what role exosomes play in the aggregation and/or clearance of Aβ. Exosomes have been implicated in the extracellular enzymatic degradation of Aβ (Bulloj et al., 2010) and in contrast, are reported to promote Aβ fibrillization and clearance by microglia (Yuyama et al., 2012). Our laboratory reported that cultured primary astrocytes secrete exosomes in response to Aβ exposure, a process dependent upon ceramide generation by neutral sphingomyelinase 2 (nSMase2) (Wang et al., 2012), which suggests that exosome secretion is upregulated during AD. Other work has shown that glia preferentially take up oligomeric Aβ compared to fibrils (Nielsen et al., 2010), suggesting that Aβ aggregation interferes with efficient clearance. In this study, we show that exosomes promote Aβ aggregation and by extension, plaque formation *in vivo*. Inhibition of nSMase2 with GW4869 (Luberto et al., 2002) in the 5XFAD mouse blocks exosome secretion to reduce plaque formation and decrease the overall brain amyloid load.

2. Methods

2.1. Animals and GW4869 administration

All experiments involving animals followed approved protocols by Georgia Regents University's Institutional Animal Care and Use Committee. Mice expressing five human mutations in APP and PS1 (B6SJL-Tg[APP*K670N*M671L*I716V*V717I, PSEN1*M146*L286V]6799Vas/J) under neuron-specific elements of the Thy1 promoter were purchased from The Jackson Laboratory and crossed to wildtype C57Bl/6 mice to generate offspring hemizygous for the APP and PS1 transgenes. These mice predominately generate Aβ1-42 that accumulates in plaques beginning at 2 months of age. GW4869 (N,N'-Bis[4-(4,5-dihydro-1H-imidazol-2-yl)phenyl]-3,3'-p-phenylene-bis-acrylamide dihydrochloride; molecular weight 577.5 g/mol; Cayman Chemical) was maintained in DMSO at 8 mg/mL. Two month old mice were injected intraperitoneally with 200 μl of 0.3 mg/mL GW4869 in 0.9% normal saline (60 μg/mouse; 2-2.5 μg/g body weight) or 200 μl of 3.75% DMSO saline control every 48 h for six weeks (21 injections total). Mice were sacrificed 24 h after the final injection. No obvious behavioral or health problems were observed during treatment.

2.2. Sample preparation

Mice were sacrificed by decapitation following isoflurane sedation. Blood was drained for serum collection, and brains were removed and cut mid-sagitally. One half was frozen on dry ice and stored at −80°C for Aβ1-42 ELISA and ceramide analyses, and the other was fixed in 4% p-formaldehyde/PBS for cryosectioning. Hemibrains were homogenized in cold NaCl (50 mM, 1 mL/100 mg tissue). To extract soluble Aβ, diethylamine (DEA) was added to a final concentration of 0.2%, and the samples were centrifuged at 100,000 xg for 1 h at 4°C. 100 μL of 0.5M Tris (pH 6.8) was added to 1 mL supernatant to neutralize DEA, and samples were diluted and used directly for ELISA. To extract total Aβ, 200 μL of homogenate was added to 440 μL cold formic acid (88%, Fisher Scientific), and samples were sonicated for 1 minute on ice and centrifuged at 150,000 xg for 1 h at 4°C. 100 μL of supernatant was diluted into 2 mL of neutralization solution (1M Tris base, 0.5 M Na_2HPO_4, 0.05% NaN_3) and further diluted for ELISA. ELISA was performed with 50 μL sample according to the manufacturer's instructions (Life Technologies human Aβ1-42 ELISA kit).

2.3. Characterization of ceramide using GC-MS

Fatty acyl composition of ceramide was analyzed as methyl esters while the base composition was characterized as trimethylsilyl-derivative (Dasgupta and Hogan, 2001). Briefly, a defined amount of ceramide solution was transferred to a screw-cap tube, dried under nitrogen, and hydrolyzed with methanol-water-HCl 29:4:3 (v/v) (Gaver and Sweeley, 1965) at 80°C for 18h in a sealed tube. The mixture of free fatty acids and fatty acid methyl esters (FAME) was recovered by partitioning with hexane and re-methylated using 1M methanolic HCl for 16h-18h at 80°C, and the recovered base from the methanol-HCl layer was analyzed as TMS-derivative after N-acetylation (Pritchard and Todd, 1977). FAME was analyzed using the GC-MS conditions described above but with the temperature program extended to 300°C to ensure elution and detection through the 2-OH, C26 FAME derivatives (Laine et al., 1974). EI-MS detector acquired 50–500 amu for fatty acid analysis.

2.4. Primary cell culture and exosome isolation

Mixed glial cells were isolated from brains of 1 day old wildtype mouse pups. Brains were dissociated in PBS containing 0.1M glucose, passed through a 40 μm filter, and plated in T-25 flasks in DMEM (Cellgro) containing 10% fetal bovine serum (Atlanta Biologicals, Premium Select) and GlutaGRO (Cellgro). After 7 days, mixed glial cultures were dissociated, labeled with anti-CD11b microbeads (Miltenyi Biotec) and passed through a magnetic column to remove microglia. Astrocytes were plated on 100 mm dishes and grown to confluency for exosome collection. Treatment of cells with GW4869 (or DMSO control) and/or Aβ25-35 (AnaSpec) to induce exosome secretion and Aβ1-42 uptake experiments were done with phenol red- and serum-free DMEM (Cellgro). Primary neurons were isolated from E16.5 mouse cortices following 30 min trypsinization and trituration with a flame-polished Pasteur pipet. Neurons were plated on polyethyleneimine coated T-25 flasks and maintained 7 days in Neurobasal medium with B27 supplement (Life Technologies) prior to GW4869 treatment. To harvest exosomes, conditioned media were centrifuged (4°C) at 300xg for 10 minutes, 1000xg for 10 minutes and 20,000xg for 30 minutes to remove dead cells, cellular debris and larger microvesicles, respectively. Supernatant was

then centrifuged (4°C) at 110,000xg for 2 h. Exosome pellets were resuspended in SDS sample buffer (western blot analysis), Tris-buffered saline (TBS; aggregation assays), or serum-free DMEM (amyloid uptake assays). Serum samples from mice were diluted in PBS, and exosomes were isolated as described for culture medium. To isolate exosomes from brain tissues, we followed the method described by Perez-Gonzalez et al. (Perez-Gonzalez et al., 2012).

2.5. Amyloid aggregation assay

Hexofluoroisopropanol-(HFIP) treated human Aβ1-42 (AnaSpec) was dissolved in 0.1% ammonia, aliquoted, and frozen at −80°C. Exosomes were suspended in TBS (50 mM Tris, 150 mM NaCl, pH 7.5) to which rabbit IgG or anti-ceramide was added (4 μg/mL). Monomeric Aβ1-42 was added to a final concentration of 20 μM, and the samples were incubated at 37°C for 18 h on a shaking platform at 100 rpm. Samples were centrifuged at 20,000 xg to pellet Aβ aggregates and washed 3 times before dissolving pellets in 10 μl cold formic acid. Samples were then processed as described above for brain Aβ and analyzed by ELISA.

2.6. Amyloid uptake assay

Mixed glial cultures were passed to 12-well plates and grown to confluency. Exosomes were resuspended in serum-free DMEM to which unlabeled Aβ1-42 (ELISA) was added followed by a 1 h incubation period at 37°C with varying amounts of exosomes (5-15 μg protein). Exosome-Aβ mixtures or Aβ alone (200 μL) were then added to mixed glial cultures in 800 μL serum-free DMEM for 18 h. The final Aβ1-42 concentration was 0.5 μM (ELISA). For ELISA assays, cells were washed 3 times with PBS and solubilized with 100 μL formic acid and processed as described for brain Aβ. Protein content was measured by the RC/DC assay method (BioRad).

2.7. Exosome injection and amyloid labeling in brain sections

To directly label plaques, brain cryosections were washed for 1 min each in 70% and 80% ethanol and then incubated with 1% thioflavin S in 80% ethanol for 15 min. Slides were then washed for 1 min each in 80% and 70% ethanol, rinsed in deionized water, and mounted with Fluoroshield containing DAPI (Sigma). For exosome injection, donor astrocytes were labeled with Vybrant CM-DiI (5 μL/mL DMEM) for 1 h followed by 40 μM Aβ25-35 for 3 days. DiI-labeled exosomes were isolated as described above, resuspended in sterile PBS, and injected into the brains 10-day-old 5XFAD mice. Mice were sacrificed 48 h later, and the brains fixed in 4% p-formaldehyde/PBS. For immunohistochemistry, brain cryosections were permeabilized with 0.2% Triton X-100 in PBS for 10 minutes. Amyloid plaques were labeled with 1 μg/mL Aβ1-42 ABfinity™ recombinant rabbit monoclonal antibody (Life Technologies) in PBS plus 0.5% BSA. The secondary antibody AlexaFluor488-donkey anti-rabbit IgG (Jackson Immunoresearch) used at 1μg/mL in PBS plus 0.5% BSA. Confocal fluorescence microscopy was performed with an LSM 510 confocal scanning microscope using LSM 510 Meta 3.2 software for image acquisition. Images obtained with secondary antibody only were used as negative controls representing the background intensity in a particular laser channel.

2.8. Statistical analysis

To analyze thioflavin-labeled amyloid plaques, brain sections were imaged under epifluorescence microscopy. Cortical images were acquired from 3 sections per animal (4-5 images per section), background subtracted, and analyzed with ImageJ for plaque number, total plaque area, and average plaque area. Data for amyloid aggregation and amyloid uptake assays were analyzed by one-way ANOVA with Bonferroni post-hoc test. All data from control- and GW4869-treated mice were analyzed by unpaired t-test with Welch's correction. Animal data were collected with samples blinded to the person performing the analysis. Results showing $p < 0.05$ were considered to be statistically significant for all experiments.

3. Results

3.1. Astrocyte-derived exosomes promote Aβ aggregation and interfere with uptake by glia

Because exosomes derived from N2A neuroblastoma cells were able to promote Aβ aggregation *in vitro* (Yuyama et al., 2012), we tested whether astrocyte-derived exosomes held this property. Monomeric Aβ1-42 (20 μM) was incubated at 37°C for 18 h with or without exosomes collected from astrocyte-conditioned medium. Exosomes stimulated the aggregation of Aβ, visible as a pellet following centrifugation, approximately 20-fold over Aβ incubated alone. Inclusion of rabbit anti-ceramide IgG (Krishnamurthy et al., 2007) with exosomes blocked Aβ aggregation (Fig. 1A), suggesting that ceramide was critical in exosome-mediated Aβ aggregation. We next tested the effect of astrocyte-derived exosomes on the uptake of Aβ1-42 by primary mixed glial cultures (nearly 1:1 ratio of astrocytes to microglia). Pre-incubation of Aβ1-42 with exosomes for 1 h prior to addition to glial cultures resulted in 30–60% reduction in cellular Aβ uptake, depending on the amount of exosomes added (Fig. 1B). We confirmed the reduced uptake of Aβ in the presence of exosomes by FACS analysis using HiLyte488-labeled Aβ1-42 and anti-GLAST-APC to distinguish astrocytes and microglia. Addition of exosomes to cultures resulted in 16–25% fewer astrocytes and 15–18% fewer microglia being positive for using HiLyte488-labeled Aβ1-42 (not shown). Confocal microscopy confirmed that both astrocytes and microglia could take up Aβ1-42-HiLyte488, often mutually exclusive of exosome uptake (Fig. S1).

To test whether exosomes could stimulate aggregation of Aβ *in vivo*, we injected Vybrant CM-DiI-labeled exosomes into 10-day old 5XFAD pups that have not yet developed plaques (Fig. 2E) but have detectable Aβ1-42 by ELISA (not shown). In brains receiving exosome injections, we detected Aβ1-42 above background levels by immunohistochemistry at the site of injections (Fig. 2B,D) but not in sham injected brains (0.01% DiI in PBS; Fig. 2A) or contralateral regions (Fig. 2C), indicating that Aβ aggregation is induced by exosomes in vivo. Fig. 2F shows immunolabeled plaques from a 4-month-old 5XFAD mouse brain as a positive control. In preliminary studies, we also injected exosomes into wildtype mouse pups but were not able to detect any plaques or evidence of endogenous Aβ aggregation with Aβ-specific antibodies (not shown). These results suggest that, as amyloid levels rise in aged individuals, exosomes can trigger aggregation events that contribute to plaque deposition.

3.2. GW4869 inhibition of nSMase2 blocks exosome secretion in vivo and decreases brain ceramide levels

We previously reported that Aβ causes apoptosis and stimulates exosome secretion in primary astrocytes, both of which were blocked in astrocytes from nSMase2-deficient mice (Wang et al., 2012). We tested GW4869 on primary cultured wildtype neurons and astrocytes. In agreement with published data (Yuyama et al., 2012), GW4869 reduced exosome secretion from primary neurons (Fig. 3A) as well as astrocytes treated with Aβ25-35 (Fig. 3B) with no loss of viability at 10–40 μM (not shown). Because GW4869 prevented exosome secretion from neurons and astrocytes, we reasoned that it could reduce exosome secretion in the brain. We first tested whether GW4869 could lower brain exosome secretion in wildtype mice by giving intraperitoneal injections of 100 μg GW4869 (~4 μg/g) daily for 5 days and processing brains for exosome isolation as described (Perez-Gonzalez et al., 2012). We detected exosomal markers Alix and Tsg101 in the 0.55 and 0.80 M fractions following ultracentrifugation on a discontinuous sucrose density gradient (Fig. 3C). Compared to controls, brain exosomes from GW4869-injected mice had reduced levels of Alix and Tsg101as detected by western blot analysis (Fig. 3D) as well as reduced overall protein content (Fig. 3E) in the 0.55 and 0.80 M fractions following sucrose density gradient centrifugation.

We then moved to an AD mouse model to evaluate the potential of extended GW4869 treatment on amyloid levels and neuritic plaques. We chose a strain that expresses 5 familial human APP and PS1 AD mutations (5XFAD) that primarily produce Aβ1-42 with plaques forming as early as 2 months of age (Oakley et al., 2006). In this study, we were interested in the effect of exosomes on initial plaque formation. Therefore, we administered 60 μg GW4869 (~2.5 μg/g) to hemizygous 5XFAD mice every 48 h, beginning injections at 2 months of age for a total of 6 weeks. Mice treated with GW4869 did not exhibit noticeable behavioral or physiological problems, and body mass and serum LDH levels were not different from controls (Fig. S2). We determined whether extended GW4869 treatment reduced exosome secretion *in vivo*. We compared the exosome content in serum of these mice, as it has been found to be a good indicator for abnormal processes in various tissues (Bala et al., 2012; Khan et al., 2012; Skog et al., 2008). GW4869-treated mice showed reduced levels of serum exosomes compared to controls, using Alix as an approximation of total exosome levels (Fig. 3F). Consistently, serum exosome protein levels from wildtype mice given 100 μg GW4869 daily for 5 days to examine brain exosome levels (Fig. 3D,E) were also lower than control mice (Fig. 3G). We also observed that administration of GW4869 resulted in a decrease in the levels of several ceramides (C16:0, C18:0, C22:0, and C24:0) as determined by GC-MS (Fig. 3H).

3.3. Treatment of 5XFAD mice with GW4869 reduces amyloid burden

We next used ELISA to analyze the levels of soluble and total Aβ1-42 in untreated and GW4869-treated 5XFAD mouse brains. The mean concentration of soluble Aβ1-42 in males was ~60% of that in females, but differences in mean levels of soluble Aβ1-42 were not statistically significant between control and GW4869-treated mice when sexes were analyzed together (Fig. 4A) or separately (Fig. 4B,C). However, the mean concentration of total brain Aβ1-42 (soluble and plaque) was reduced by 25% following GW4869 treatment

for 6 weeks (Fig. 4D, both sexes). When sexes were analyzed separately, we found that males had the strongest response to GW4869 with a 40% decrease in total Aβ1-42 levels (Fig. 4E). Females also showed a ~20% decrease following GW4869 treatment although this difference was not statistically significant (Fig. 4F).

We analyzed brain sections from control and GW4869-treated mice (Fig. S3) to determine the number of cortical plaques and total plaque area per imaged field of view (~0.35 mm^2) as well as the average plaque size. We found significant decreases following GW4869 treatment of total plaque area and plaque number per image field (Fig. 4G-L) independent of whether sexes were analyzed together or separately. However, there were no differences between groups with respect to average individual plaque area (Fig. 4M-O). The range of the histochemical plaque data sets was large as several slides from each animal were scored (15 per mouse) to account for possible areas of sparse or high plaque density. Taken together, these data show that GW4869 treatment of 5XFAD mice results in lower brain ceramide concentration and serum exosome levels, which was also associated with lower levels of Aβ1-42 and plaque burden.

4. Discussion

The present study reveals nSMase2 as a novel potential therapeutic target in the treatment of AD. One of the hallmarks of AD progression is chronic neuroinflammation (Broussard et al., 2012). Amyloid peptides activate astrocytes and microglia, which secrete pro-inflammatory cytokines such as IL-1β and TNF-α (Meda et al., 1995; Sheng et al., 1996) that mediate activation of SMases to generate ceramide, which can lead to apoptosis (Ariga et al., 1998; Rybakina et al., 2001). Moreover, nSMase appears to be upregulated during the normal aging process (Crivello et al., 2005; Rutkute et al., 2007) and has been shown to mediate cell death in neurons in AD cell culture models (Jana and Pahan, 2010; Malaplate-Armand et al., 2006). Therefore, in addition to blocking exosome-mediated plaque formation, inhibition of nSMase2 may reduce neuroinflammation that occurs during AD progression as well as preventing apoptosis of neurons and astrocytes.

We previously reported that activated primary cultured astrocytes release pro-apoptotic exosomes in response to challenge with Aβ (Wang et al., 2012). Exosomes from N2a neuroblastoma and BV-2 microglial cells have also been reported to promote degradation of Aβ through proteolysis via exosome-associated insulin degrading enzyme (IDE) (Bulloj et al., 2010; Tamboli et al., 2010), which implies that exosomes are important for Aβ physiological clearance. In contrast, IDE was also found to promote time-dependent oligomerization of Aβ *in vitro* under physiological conditions, possibly through one of its Aβ-degradation products (Qiu et al., 1998). In addition, N2A-derived exosomes promoted Aβ fibril assembly through a GM1 ganglioside-dependent mechanism (Yuyama et al., 2012). It is also documented that microglia can take up secreted exosomes *in vitro*, which may represent one potential means of Aβ clearance from the brain (Fitzner et al., 2011; Yuyama et al., 2012). A recent study in humans showed that both AD patients and cognitively normal controls produced Aβ at a similar rate while AD patients had an impaired clearance rate (Mawuenyega et al., 2010). While it is unknown if AD patients have

an elevated level of brain-derived exosomes, it is reasonable to hypothesize that exosomes in the presence of excess Aβ may contribute to seeding neuritic plaques.

Many published reports demonstrate that Aβ aggregation is influenced by a variety of membrane lipids (Terzi et al., 1995) including phospholipids (McLaurin and Chakrabratty, 1997; Hane et al., 2011), sphingomyelin (Devanathan et al., 2006), GM1 ganglioside (Yanagisawa et al., 1995), and cholesterol (Yanagisawa and Matsuzaki, 2002). Additionally, model liposomes have been used to study Aβ aggregation, further implicating cholesterol and GM1 in the process of fibrillization (Tashima et al., 2004). We did not extend our study through the injection of synthetic liposomes or free lipids due to abundance of previously published work and unlikely *in vivo* relevance of such synthetic vesicles. It is, however, interesting to note that the Aβ aggregation property of exosomes was abrogated by blocking GM1 with cholera toxin and also by removal of glycosphingolipids oligosaccharides with endoglycoceramidase (Yuyama et al., 2012; Yuyama et al., 2008). While we were able to prevent exosome-induced Aβ aggregation with anti-ceramide antibodies, it is more likely that this reversal was due to general steric blocking effect than a specific amyloid-ceramide interaction. It was recently reported that ceramide liposomes had no observable Aβ binding properties, but the observation that senile plaques were enriched with ceramides and sphingomyelinases (Panchal et al., 2014) may be explained by the presence of exosomes as potential seeds for Aβ aggregation (Rajendran et al., 2006; Yuyama et al., 2008).

We chose the 5xFAD mouse model to address how exosomes influence amyloid aggregation/plaque formation and Aβ clearance. While the scope of this study only peripherally addresses amyloid clearance *in vitro*, we provide evidence that exosomes promote aggregation of Aβ1-42, which is the primary peptide produced in the 5xFAD model (Oakley et al., 2006). However, this model is not representative of typical age-related sporadic AD. The five mutations in the APP and PS1 proteins are more representative of familial AD albeit with much more rapid production and accumulation of Aβ1-42 due to the additive effects of these mutations (Eckman et al., 1997; Citron et al., 1998). The 5xFAD mice do not present with neurofibrillary tangles characteristic of AD, but this is not surprising as tangle pathology is not reported for other APP or APP/PS1 transgenic mice (Oakley et al., 2006; Sturchler-Pierrat et al., 1997). Since the current study focused solely on exosome influence on Aβ levels and aggregation, the 5xFAD is a sufficient model in which to study these effects. Because the 5xFAD phenotype is so robust in its amyloid production (i.e., plaques detectable after 2 months), our data showing a reduction in plaque burden in this model suggest a potentially stronger response to nSMase-2 inhibition in a mouse model such as APP/PS1.

To test whether GW4869 had an effect on ceramide levels and exosome production, we determined the relative levels of different ceramide species and harvested exosomes from serum. With the exception of C20:0, we found that GW4869-treated mice had statistically lower levels of each major ceramide species, including C18:0, which we previously found to be increased in astrocytes treated with Aβ as well as enriched in exosomes secreted by these astrocytes (Wang et al., 2012). Consistent with these data, we also found that GW4869-treated mice had reduced amount of exosomes in their serum based on western blot analysis for the exosome marker Alix. Moreover, individual mice with the lowest levels of serum

exosomal Alix were the same mice with smallest cortical plaque load, further supporting that a reduction in the amount of exosomes correlates with reduction in Aβ plaques. These data are consistent with other published works that identify ceramide as a key regulator of Aβ biogenesis (Costantini et al., 2005; Puglielli et al., 2003) although nSMase2 inhibition was not part of these studies.

There are other published studies that report use of GW4869 to effectively inhibit nSMase2 *in vivo*. Intraperitoneal administration of GW4869 for 21 days at 1.25 μg/g mouse body weight was able to cross the blood-brain barrier to inhibit nSMase2, alter brain and blood sphingolipid content, and affect spatial memory (Tabatadze et al., 2010). Another study using a lower dose (1 μg/g) twice weekly for 5 weeks was able to prevent the neointimal thickening of transplanted mesenteric arteries treated with an anti-human leukocyte antigen antibody (Galvani et al., 2011). With respect to inhibition of exosome secretion *in vivo*, GW4869 (1.25 μg/g) treatment for 5 days reduced lung multiplicities following Lewis lung carcinoma cell injection, which was reversed by a single tail-vein injection of Lewis lung carcinoma cell-derived exosomes expressing specific miRNA species (Fabbri et al., 2012). Though behavioral test was out of the scope of this study of early plaque formation, we did not notice any immediately obvious difference between DMSO- and GW4869-injected mice during the course of the treatment. Additionally, our use of a higher dose of GW4869 (~2.5 μg/g) compared to the cited studies suggests that GW4869 may have a low toxicity at levels needed to achieve a biological effect from nSMase2 inhibition. This is the first study, to our knowledge, to show that pharmacological inhibition of nSMase2 reduces amyloid burden and plaque load in AD brains *in vivo*, indicating that this drug intervention may offer new treatment options for AD.

Supplementary Material

Refer to Web version on PubMed Central for supplementary material.

Acknowledgments

This work was funded by the National Institutes of Health R01-AG034389 to E.B. The funders had no role in study design, data collection and analysis, decision to publish, or preparation of the manuscript. We thank C. Wakade and J. Pihkala for additional technical assistance. We are grateful to Katarzyrna Pituch (supervisor Dr. Irene Givogri), University of Illinois at Chicago, for assistance with the exosome isolation from brain. We thank the imaging core facility (under supervision of Drs. Ana and Paul McNeil) for help with confocal microscopy. We also thank the Institute of Molecular Medicine and Genetics (Dr. Lin Mei, director), Georgia Regents University, Augusta, GA, for institutional support.

References

Ariga T, Jarvis WD, Yu RK. Role of sphingolipid-mediated cell death in neurodegenerative diseases. J Lipid Res. 1998; 39:1–16. [PubMed: 9469581]

Bala S, Petrasek J, Mundkur S, Catalano D, Levin I, Ward J, Alao H, Kodys K, Szabo G. Circulating microRNAs in exosomes indicate hepatocyte injury and inflammation in alcoholic, drug-induced, and inflammatory liver diseases. Hepatology. 2012; 56:1946–1957. [PubMed: 22684891]

Bellingham SA, Guo BB, Coleman BM, Hill AF. Exosomes: vehicles for the transfer of toxic proteins associated with neurodegenerative diseases? Front Physiol. 2012; 3:124. [PubMed: 22563321]

Bertram L, Tanzi RE. Thirty years of Alzheimer's disease genetics: the implications of systematic meta-analyses. Nat Rev Neurosci. 2008; 9:768–778. [PubMed: 18802446]

Bird TD. Genetic aspects of Alzheimer disease. Genet Med. 2008; 10:231–239. [PubMed: 18414205]

Broussard GJ, Mytar J, Li RC, Klapstein GJ. The role of inflammatory processes in Alzheimer's disease. Inflammopharmacology. 2012; 20:109–126. [PubMed: 22535513]

Bulloj A, Leal MC, Xu H, Castano EM, Morelli L. Insulin-degrading enzyme sorting in exosomes: a secretory pathway for a key brain amyloid-beta degrading protease. J Alzheimers Dis. 2010; 19:79–95. [PubMed: 20061628]

Citron M, Eckman CB, Diehl TS, Corcoran C, Ostaszewski BL, Xia W, Levesque G, St. George Hyslop P, Younkin SG, Selkoe DJ. Additive effects of PS1 and APP mutations on secretion of the 42-residue amyloid beta-protein. Neurobiol Dis. 1998; 5:107–116. [PubMed: 9746908]

Costantini C, Weindruch R, Della Valle G, Puglielli L. A TrkA-to-p75NTR molecular switch activates amyloid beta-peptide generation during aging. Biochem J. 2005; 391:59–67. [PubMed: 15966860]

Cramer PE, Cirrito JR, Wesson DW, Lee CY, Karlo JC, Zinn AE, Casali BT, Restivo JL, Goebel WD, James MJ, Brunden KR, Wilson DA, Landreth GE. ApoE-directed therapeutics rapidly clear beta-amyloid and reverse deficits in AD mouse models. Science. 2012; 335:1503–1506. [PubMed: 22323736]

Crivello NA, Rosenberg IH, Dallal GE, Bielinski D, Joseph JA. Age-related changes in neutral sphingomyelin-specific phospholipase C activity in striatum, hippocampus, and frontal cortex: implication for sensitivity to stress and inflammation. Neurochem Int. 2005; 47:573–579. [PubMed: 16140422]

Dasgupta S, Hogan EL. Chromatographic resolution and quantitative assay of CNS tissue sphingoids and sphingolipids. J Lipid Res. 2001; 42:301–308. [PubMed: 11181761]

Devanathan S, Salamon Z, Lindblom G, Gröbner G, Tollin G. Effects of sphingomyelin, cholesterol and zinc ions on the binding, insertion and aggregation of the amyloid Abeta(1-40) peptide in solid-supported lipid bilayers. FEBS J. 2006; 273:1389–1402. [PubMed: 16689927]

Eckman CB, Mehta ND, Crook R, Perez-tur J, Prihar G, Pfeiffer E, Graff-Radford N, Hinder P, Yager D, Zenk B, Refolo LM, Prada CM, Younkin SG, Hutton M, Hardy J. A new pathogenic mutation in the APP gene (I716V) increases the relative proportion of A beta 42(43). Hum Mol Genet. 1997; 6:2087–2089. [PubMed: 9328472]

Fabbri M, Paone A, Calore F, Galli R, Gaudio E, Santhanam R, Lovat F, Fadda P, Mao C, Nuovo GJ, Zanesi N, Crawford M, Ozer GH, Wernicke D, Alder H, Caligiuri MA, Nana-Sinkam P, Perrotti D, Croce CM. MicroRNAs bind to Toll-like receptors to induce prometastatic inflammatory response. Proc Natl Acad Sci U S A. 2012; 109:E2110–E2116. [PubMed: 22753494]

Fitzner D, Schnaars M, van Rossum D, Krishnamoorthy G, Dibaj P, Bakhti M, Regen T, Hanisch UK, Simons M. Selective transfer of exosomes from oligodendrocytes to microglia by macropinocytosis. J Cell Sci. 2011; 124:447–458. [PubMed: 21242314]

Galvani S, Trayssac M, Auge N, Thiers JC, Calise D, Krell HW, Sallusto F, Kamar N, Rostaing L, Thomsen M, Negre-Salvayre A, Salvayre R. A key role for matrix metalloproteinases and neutral sphingomyelinase-2 in transplant vasculopathy triggered by anti-HLA antibody. Circulation. 2011; 124:2725–2734. [PubMed: 22082680]

Gaver RC, Sweeley CC. Methods for Methanolysis of Sphingolipids and Direct Determination of Long-Chain Bases by Gas Chromatography. J Am Oil Chem Soc. 1965; 42:294–298. [PubMed: 14279115]

Geekiyanage H, Upadhye A, Chan C. Inhibition of serine palmitoyltransferase reduces Abeta and tau hyperphosphorylation in a murine model: a safe therapeutic strategy for Alzheimer's disease. Neurobiol Aging. 2013; 34:2037–2051. [PubMed: 23528227]

Haass C, Lemere CA, Capell A, Citron M, Seubert P, Schenk D, Lannfelt L, Selkoe DJ. The Swedish mutation causes early-onset Alzheimer's disease by betasecretase cleavage within the secretory pathway. Nat Med. 1995; 1:1291–1296. [PubMed: 7489411]

Hane F, Drolle E, Gaikwad R, Faught E, Leonenko Z. Amyloid-b aggregation on model lipid membranes: an atomic force microscopy study. J Alzheimers Dis. 2011; 26:485–494. [PubMed: 21694459]

Jana A, Pahan K. Fibrillar amyloid-beta-activated human astroglia kill primary human neurons via neutral sphingomyelinase: implications for Alzheimer's disease. J Neurosci. 2010; 30:12676–12689. [PubMed: 20861373]

Khan S, Jutzy JM, Valenzuela MM, Turay D, Aspe JR, Ashok A, Mirshahidi S, Mercola D, Lilly MB, Wall NR. Plasma-derived exosomal survivin, a plausible biomarker for early detection of prostate cancer. PLoS One. 2012; 7:e46737. [PubMed: 23091600]

Krishnamurthy K, Dasgupta S, Bieberich E. Development and characterization of a novel anti-ceramide antibody. J Lipid Res. 2007; 48:968–975. [PubMed: 17210985]

Laine RA, Young ND, Gerber JN, Sweeley CC. Identification of 2-hydroxy fatty acids in complex mixtures of fatty acid methyl esters by Mass chromatography. Biomed Mass Spectrom. 1974; 1:10–14. [PubMed: 4433710]

Liu B, Frost JL, Sun J, Fu H, Grimes S, Blackburn P, Lemere CA. MER5101, a novel Abeta1-15:DT conjugate vaccine, generates a robust anti-Abeta antibody response and attenuates Abeta pathology and cognitive deficits in APPswe/PS1DeltaE9 transgenic mice. J Neurosci. 2013; 33:7027–7037. [PubMed: 23595760]

Luberto C, Hassler DF, Signorelli P, Okamoto Y, Sawai H, Boros E, Hazen-Martin DJ, Obeid LM, Hannun YA, Smith GK. Inhibition of tumor necrosis factor-induced cell death in MCF7 by a novel inhibitor of neutral sphingomyelinase. J Biol Chem. 2002; 277:41128–41139. [PubMed: 12154098]

Malaplate-Armand C, Florent-Bechard S, Youssef I, Koziel V, Sponne I, Kriem B, Leininger-Muller B, Olivier JL, Oster T, Pillot T. Soluble oligomers of amyloid-beta peptide induce neuronal apoptosis by activating a cPLA2-dependent sphingomyelinase-ceramide pathway. Neurobiol Dis. 2006; 23:178–189. [PubMed: 16626961]

Mawuenyega KG, Sigurdson W, Ovod V, Munsell L, Kasten T, Morris JC, Yarasheski KE, Bateman RJ. Decreased clearance of CNS beta-amyloid in Alzheimer's disease. Science. 2010; 330:1774. [PubMed: 21148344]

McLaurin J, Chakrabartty A. Characterization of the interactions of Alzheimer beta-amyloid peptides with phospholipid membranes. Eur J Biochem. 1997; 245:355–363. [PubMed: 9151964]

Meda L, Cassatella MA, Szendrei GI, Otvos L Jr, Baron P, Villalba M, Ferrari D, Rossi F. Activation of microglial cells by beta-amyloid protein and interferongamma. Nature. 1995; 374:647–650. [PubMed: 7715705]

Nielsen HM, Mulder SD, Belien JA, Musters RJ, Eikelenboom P, Veerhuis R. Astrocytic A beta 1-42 uptake is determined by A beta-aggregation state and the presence of amyloid-associated proteins. Glia. 2010; 58:1235–1246. [PubMed: 20544859]

Oakley H, Cole SL, Logan S, Maus E, Shao P, Craft J, Guillozet-Bongaarts A, Ohno M, Disterhoft J, Van Eldik L, Berry R, Vassar R. Intraneuronal beta-amyloid aggregates, neurodegeneration, and neuron loss in transgenic mice with five familial Alzheimer's disease mutations: potential factors in amyloid plaque formation. J Neurosci. 2006; 26:10129–10140. [PubMed: 17021169]

Panchal M, Gaudin M, Lazar AN, Salvati E, Rivals I, Ayciriex S, Dauphinot L, Dargère D, Auzeil N, Masserini M, Laprévote O, Duyckaerts C. Ceramides and sphingomyelinases in senile plaques. Neurobiol Dis. 2014 In press.

Perez-Gonzalez R, Gauthier SA, Kumar A, Levy E. The exosome secretory pathway transports amyloid precursor protein carboxyl-terminal fragments from the cell into the brain extracellular space. J Biol Chem. 2012; 287:43108–43115. [PubMed: 23129776]

Pritchard DG, Todd CW. Gas chromatography of methyl glycosides as their trimethylsilyl ethers. The methanolysis and re-N-acetylation steps. J Chromatogr. 1977; 133:133–139. [PubMed: 838792]

Puglielli L, Ellis BC, Saunders AJ, Kovacs DM. Ceramide stabilizes beta-site amyloid precursor protein-cleaving enzyme 1 and promotes amyloid beta-peptide biogenesis. J Biol Chem. 2003; 278:19777–19783. [PubMed: 12649271]

Qiu WQ, Walsh DM, Ye Z, Vekrellis K, Zhang J, Podlisny MB, Rosner MR, Safavi A, Hersh LB, Selkoe DJ. Insulin-degrading enzyme regulates extracellular levels of amyloid beta-protein by degradation. J Biol Chem. 1998; 273:32730–32738. [PubMed: 9830016]

Rajendran L, Honsho M, Zahn TR, Keller P, Geiger KD, Verkade P, Simons K. Alzheimer's disease beta-amyloid peptides are released in association with exosomes. Proc Natl Acad Sci USA. 2006; 103:11172–11177. [PubMed: 16837572]

Rutkute K, Asmis RH, Nikolova-Karakashian MN. Regulation of neutral sphingomyelinase-2 by GSH: a new insight to the role of oxidative stress in aging-associated inflammation. J Lipid Res. 2007; 48:2443–2452. [PubMed: 17693623]

Rybakina EG, Nalivaeva NN, Pivanovich YU, Shanin SN, Kozinets A, Korneva EA. The role of neutral sphingomyelinase in interleukin-1beta signal transduction in mouse cerebral cortex cells. Neurosci Behav Physiol. 2001; 31:439–444. [PubMed: 11508496]

Selkoe DJ. Resolving controversies on the path to Alzheimer's therapeutics. Nat Med. 2011; 17:1060–1065. [PubMed: 21900936]

Sharples RA, Vella LJ, Nisbet RM, Naylor R, Perez K, Barnham KJ, Masters CL, Hill AF. Inhibition of gamma-secretase causes increased secretion of amyloid precursor protein C-terminal fragments in association with exosomes. Faseb J. 2008; 22:1469–1478. [PubMed: 18171695]

Sheng JG, Ito K, Skinner RD, Mrak RE, Rovnaghi CR, Van Eldik LJ, Griffin WS. In vivo and in vitro evidence supporting a role for the inflammatory cytokine interleukin-1 as a driving force in Alzheimer pathogenesis. Neurobiol Aging. 1996; 17:761–766. [PubMed: 8892349]

Skog J, Wurdinger T, van Rijn S, Meijer DH, Gainche L, Sena-Esteves M, Curry WT Jr, Carter BS, Krichevsky AM, Breakefield XO. Glioblastoma microvesicles transport RNA and proteins that promote tumour growth and provide diagnostic biomarkers. Nat Cell Biol. 2008; 10:1470–1476. [PubMed: 19011622]

Sturchler-Pierrat C, Abramowski D, Duke M, Wiederhold KH, Mistl C, Rothacher S, Ledermann B, Burki K, Frey P, Paganetti PA, Waridel C, Calhoun ME, Jucker M, Probst A, Staufenbiel M, Sommer B. Two amyloid precursor protein transgenic mouse models with Alzheimer disease-like pathology. Proc Natl Acad Sci USA. 1997; 94:13287–13292. [PubMed: 9371838]

Tabatadze N, Savonenko A, Song H, Bandaru VV, Chu M, Haughey NJ. Inhibition of neutral sphingomyelinase-2 perturbs brain sphingolipid balance and spatial memory in mice. J Neurosci Res. 2010; 88:2940–2951. [PubMed: 20629193]

Tamboli IY, Barth E, Christian L, Siepmann M, Kumar S, Singh S, Tolksdorf K, Heneka MT, Lutjohann D, Wunderlich P, Walter J. Statins promote the degradation of extracellular amyloid {beta}-peptide by microglia via stimulation of exosome-associated insulin-degrading enzyme (IDE) secretion. J Biol Chem. 2010; 285:37405–37414. [PubMed: 20876579]

Tashima Y, Oe R, Lee S, Sugihara G, Chambers EJ, Takahashi M, Yamada T. The effect of cholesterol and monosialoganglioside (GM1) on the release and aggregation of amyloid beta-peptide from liposomes prepared from brain membrane-like lipids. J Biol Chem. 2004; 279:17587–17595. [PubMed: 14709559]

Terzi E, Hölzemann G, Seelig J. Self-association of beta-amyloid peptide (1-40) in solution and binding to lipid membranes. J Mol Biol. 1995; 252:633–642. [PubMed: 7563079]

Thery C. Exosomes: secreted vesicles and intercellular communications. F1000 Biol Rep. 2011; 3:15. [PubMed: 21876726]

Trajkovic K, Hsu C, Chiantia S, Rajendran L, Wenzel D, Wieland F, Schwille P, Brugger B, Simons M. Ceramide triggers budding of exosome vesicles into multivesicular endosomes. Science. 2008; 319:1244–1247. [PubMed: 18309083]

Vassar R, Bennett BD, Babu-Khan S, Kahn S, Mendiaz EA, Denis P, Teplow DB, Ross S, Amarante P, Loeloff R, Luo Y, Fisher S, Fuller J, Edenson S, Lile J, Jarosinski MA, Biere AL, Curran E, Burgess T, Louis JC, Collins F, Treanor J, Rogers G, Citron M. Beta-secretase cleavage of Alzheimer's amyloid precursor protein by the transmembrane aspartic protease BACE. Science. 1999; 286:735–741. [PubMed: 10531052]

Wang G, Dinkins M, He Q, Zhu G, Poirier C, Campbell A, Mayer-Proschel M, Bieberich E. Astrocytes Secrete Exosomes Enriched with Proapoptotic Ceramide and Prostate Apoptosis Response 4 (PAR-4): POTENTIAL MECHANISM OF APOPTOSIS INDUCTION IN ALZHEIMER DISEASE (AD). J Biol Chem. 2012; 287:21384–21395. [PubMed: 22532571]

Yanagisawa K, Matsuzaki K. Cholesterol-dependent aggregation of amyloid beta-protein. Ann N Y Acad Sci. 2002; 977:384–386. [PubMed: 12480776]

Yanagisawa K, Odaka A, Suzuki N, Ihara Y. GM1 ganglioside-bound amyloid beta-protein (A beta): a possible form of preamyloid in Alzheimer’s disease. Nat Med. 1995; 1:1062–1066. [PubMed: 7489364]

Yuyama K, Yamamoto N, Yanagisawa K. Accelerated release of exosome-**associated** GM1 ganglioside (GM1) by endocytic pathway abnormality: another putative pathway for GM1-induced amyloid fibril formation. J Neurochem. 2008; 105:217–224. [PubMed: 18021298]

Yuyama K, Sun H, Mitsutake S, Igarashi Y. Sphingolipid-modulated Exosome Secretion Promotes Clearance of Amyloid-beta by Microglia. J Biol Chem. 2012; 287:10977–10989. [PubMed: 22303002]

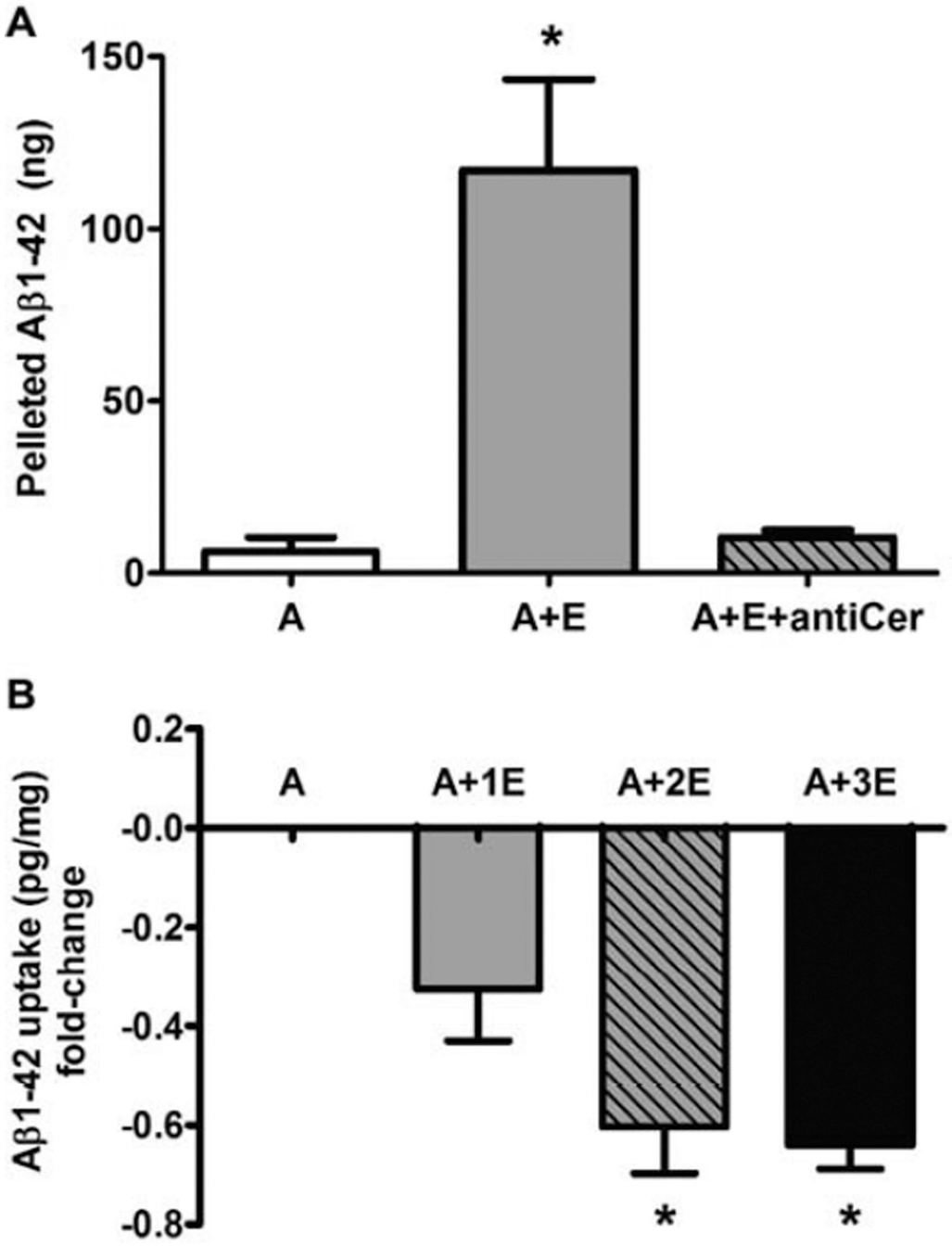

Fig. 1.

Astrocyte-derived exosomes promote aggregation and decreased uptake by mixed glial cultures of Aβ1-42 *in vitro*. (**A**) HFIP-treated human Aβ1-42 (20 μM) was incubated in 100 μL TBS (pH 7.5) alone (column A) or in the presence of exosomes (12–15 μg protein) with normal rabbit IgG (4 μg/mL; column A+E) or anti-ceramide (4 μg/mL; A+E+antiCer). Samples were centrifuged at 20,000×g after 18 h incubation at 37°C, and resulting pellets were washed and processed for Aβ1-42-specific ELISA. Data reported as mean ± SEM, n=3, *p < 0.01, ANOVA with Bonferroni post hoc test. (**B**) HFIP-treated human Aβ1-42

was incubated in serum-free DMEM alone (A) or with exosomes, 5 μg (A+1E), 10 μg (A +2E), or 15 μg (A+3E) protein, for 1 h prior to addition to mixed glial cultures for 18 h (final Aβ, 0.5 μM). Cell lysates were subjected to Aβ1-42-specific ELISA. Data are reported as fold-change based on mean ± SEM intracellular pg Aβ1-42/mg protein, n=3, *$p < 0.01$, ANOVA with Bonferroni post hoc test.

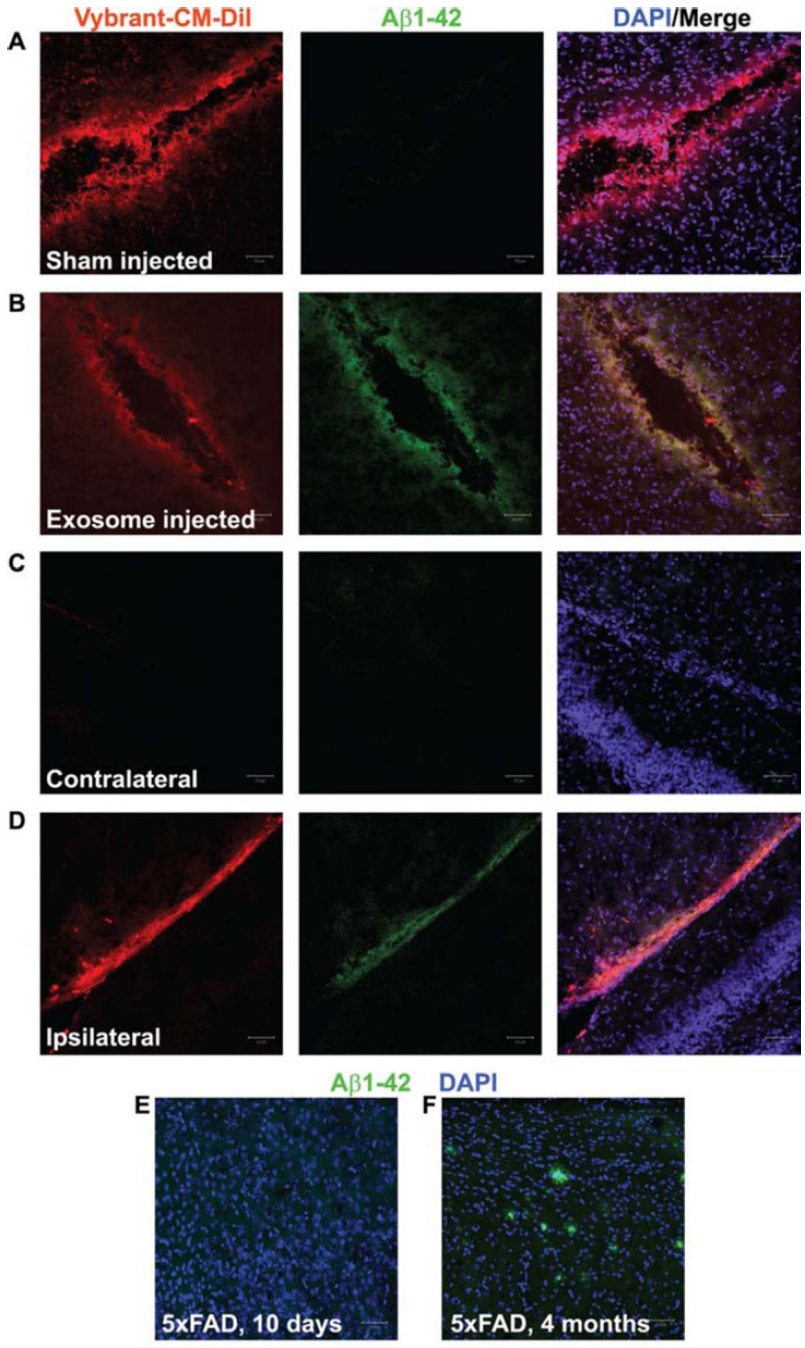

Fig. 2.

Injection of exosomes into 5xFAD mouse brains stimulates aggregation of Aβ1-42. (**A-D**) Confocal micrographs of 5xFAD mouse brain sections following sham injection (**A**, control) or injection of astrocyte-derived exosomes (**B,D**) performed on 10-day old 5xFAD pups that were sacrificed 48 h later. Exosomes were harvested from astrocytes pre-labeled with Vybrant CM-DiI (**B,D**, red) and resuspended in PBS. Control injections (**A**) contained 0.01% Vybrant CM-DiI in PBS. All sections were labeled with rabbit anti-Aβ1-42 and AlexaFluor488- anti rabbit IgG (green). Nuclei were labeled with DAPI (blue). Note that

sham-injected (**A**) and the area contralateral (**C**) to the exosome injection site (**D**) do not show an accumulation of Aβ1-42. (**E-F**) Positive and negative controls, respectively, are represented by an adult 5xFAD brain (**E**) and an uninjected 10-day old 5xFAD pup brain (**F**). Scale bars = 50 μm.

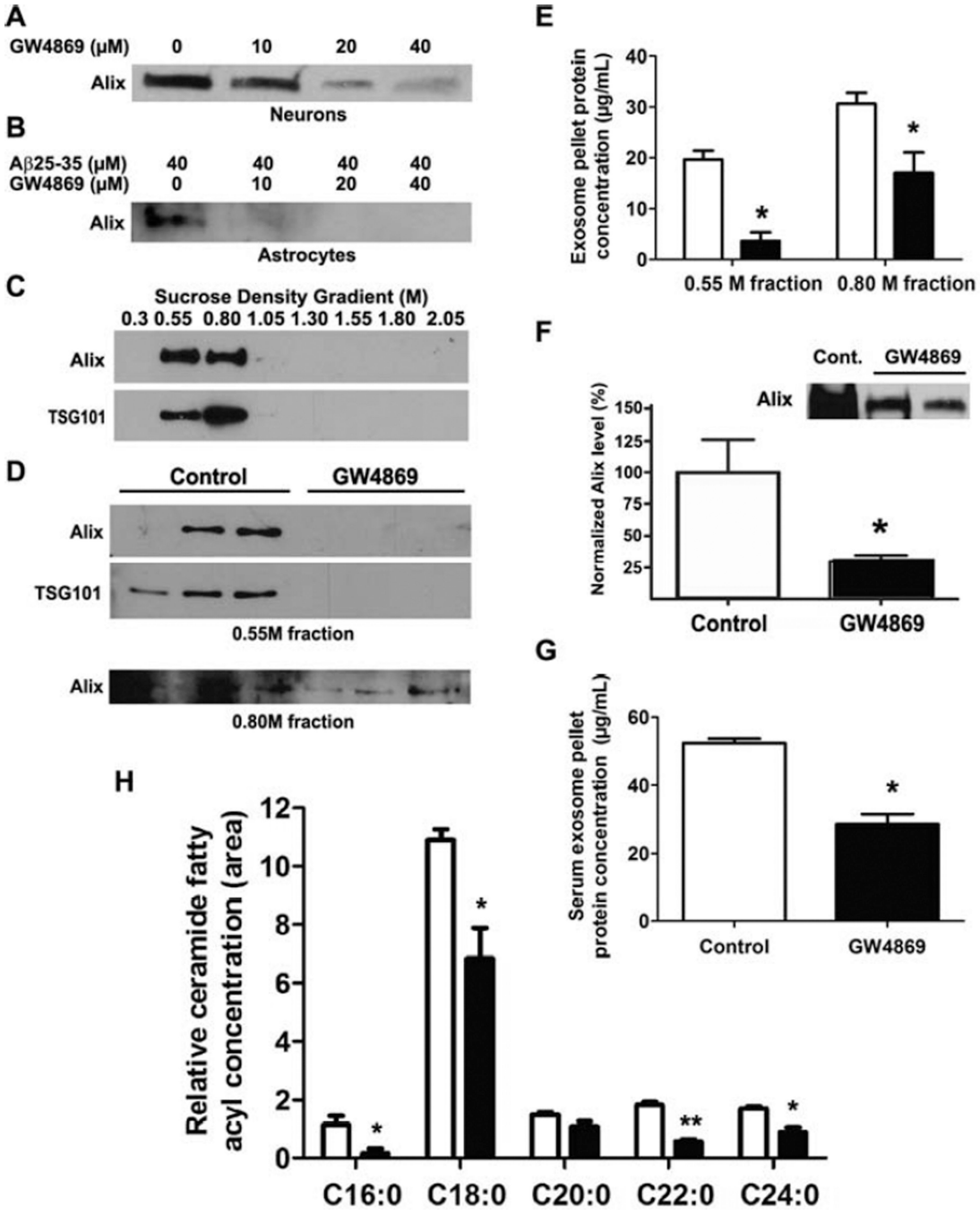

Fig. 3.

GW4869 decreases exosome secretion *in vitro* and *in vivo* and reduces brain ceramide in mice. (**A-B**) Immunoblots for Alix1 in exosomes isolated from the culture media of primary neurons treated with 0–40 μM GW4869 (**A**) and astrocytes treated with 40 μM Aβ25-35 and 0–40 μM GW4869 as indicated (**B**). (**C**) Immunoblot of exosomal markers Alix and Tsg101 from exosomes separated by discontinuous sucrose-density gradient centrifugation (0.30 - 2.05M). (**D**) Immunoblot analysis of exosomal markers Alix and Tsg101 from exosome-containing fractions (0.55M, 0.80M) following discontinuous sucrose density gradient

centrifugation. Blots show samples from 3 different control and GW4869-treated mouse brains. (**E**), Protein concentration of brain exosome pellets from samples shown (**D**) as measured by RC-DC protein assay. Data shown are mean ± SEM (n=3; *p < 0.01, unpaired t-test; open bars, control; black bars, GW4869). (**F**) Sample immunoblot for Alix1 in exosomes isolated from serum of control and GW4869-treated 5XFAD mice and densitometry of Alix1 immunoblots from serum exosomes (n=4, control; n=7, GW4869). (**G**) Protein concentration of serum exosome pellets from mice samples shown in (**D**) as measured by RC-DC protein assay. Data shown are mean ± SEM (n=3; *p < 0.001, unpaired t-test). (**H**) GC-MS analysis of relative ceramide fatty acyl chain levels from whole brains of control and GW4869-treated 5XFAD mice (age 15 weeks). Data are presented as mean ± SEM (n=3, open bars, controls; n=5, black bars, GW4869; *p < 0.05, **p < 0.01, unpaired t-test).

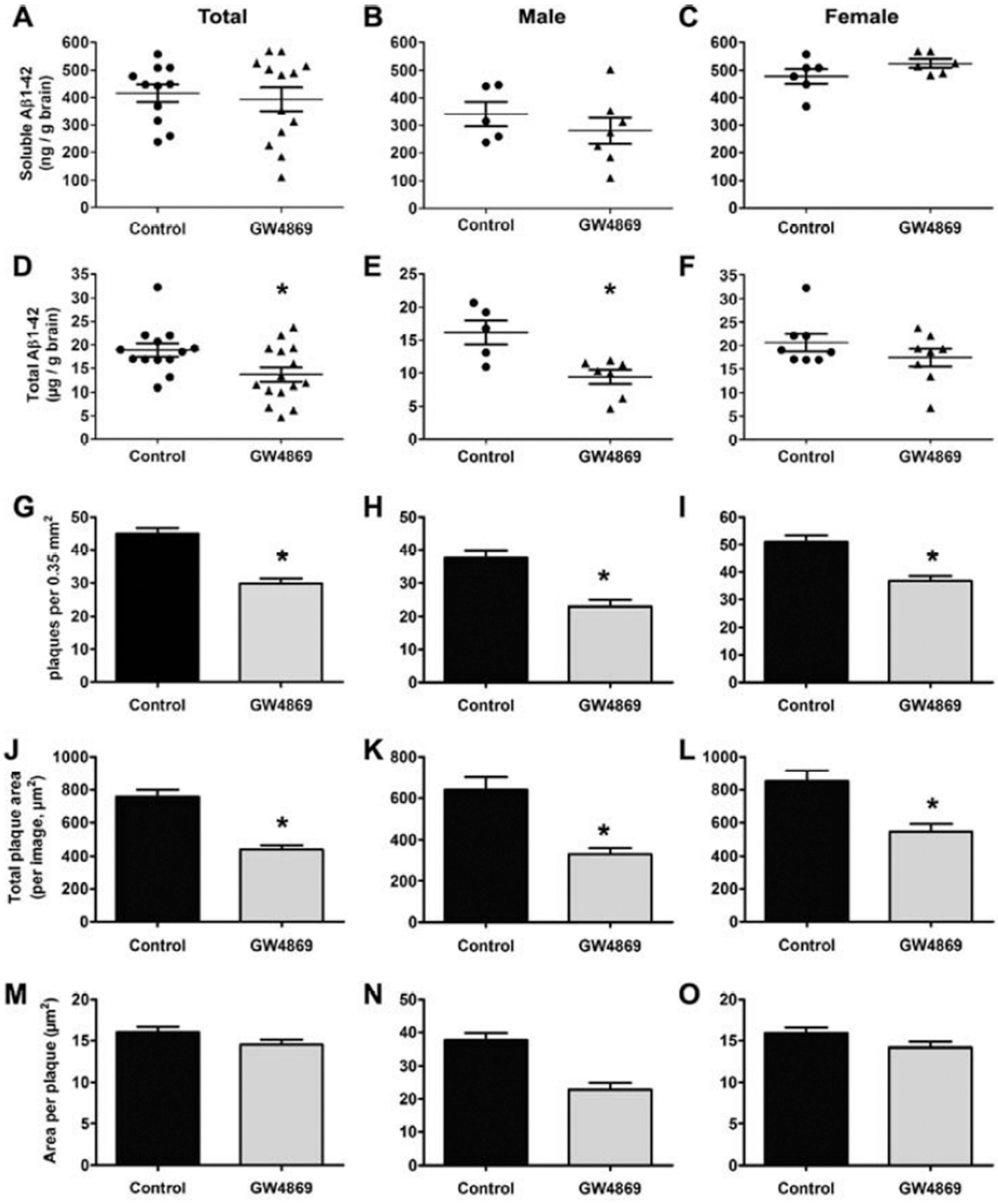

Fig. 4.

Intraperitoneal administration of GW4869 reduces total amyloid levels and plaque burden. (**A-F**) Dot plots showing soluble (**A-C**) and total (**D-F**) amyloid levels in DMSO (control)- and GW4869-treated 5XFAD mice determined by Aβ1-42 ELISA for both sexes (**A**, n=11 control, n=13 GW4869; **D**, n=13 control, n=15 GW4869), males (**B,E**, n=5 control, n=7 GW4869) and females (**C**, n=6; **F**, n=8). For **D** and **E**, *$p < 0.05$ (unpaired t-test with Welch's correction). (**G-O**) Histochemical plaque data from thioflavin S-stained brain sections of 5XFAD mice treated with DMSO (control) or GW4869. Plaques per image field

(**G-I**), total plaque area (**J-L**), and area per plaque (**M-O**) were analyzed by ImageJ for both sexes (G,J,M, n=8 control, n=9 GW4869), males (**H,K,N**, n=4 control, n=5 GW4869), and females (**I,L,O**, n=6). All data represent mean ± SEM, *p < 0.001 (unpaired t-test with Welch's correction).